

Laser Scattering from Dense Cesium Plasmas

O. L. Landen^(a) and R. J. Winfield^(b)

Imperial College, The Blackett Laboratory, London SW7 2BZ, United Kingdom

(Received 19 October 1984)

The diagnosis of a dense, cold, laser-induced, metal-vapor plasma by laser scattering techniques is reported here for the first time. The scattered spectra obtained at 90° with scattering parameter $\alpha = 1.5$ –3 showed evidence of temperature inhomogeneities and/or plasma-wave damping by electron-ion collisions. The total scattered-light intensity could be explained by inclusion of a Rayleigh scattering contribution from the cesium 6s-6p blue wing. These results also represent the most non-Debye plasmas investigated to date by scattering.

PACS numbers: 52.25.Rv

Laser scattering is a powerful, routinely used diagnostic for measuring local electron densities and temperatures in plasmas.¹ To date, scattering has been limited to hydrogen or noble-gas plasmas. The experiment presented here using cesium vapor demonstrates the feasibility of scattering in alkali-metal and alkaline-earth vapor plasmas. Such scattering would be a useful diagnostic for determining the currently contested ionization mechanisms of resonantly pumped metal vapors.² Secondly, the first detailed scattered spectra of the high-frequency “electron feature” for collective scattering ($\alpha > 1.5$) are presented. Finally, scattering in the presence of the fewest number of electrons per Debye sphere, $N_D[(4\pi/3)N_e\lambda_D^3] = 1.6$, where λ_D is the Debye length and N_e the electron density, has been achieved.

The cesium vapor was contained in a heated cross-shaped Pyrex cell with water-cooled $f/7$ ports. A Chromel-Alumel thermocouple was used to monitor the cell temperature and hence the cesium density using JANAF saturated-vapor-pressure tables.³ Cold ($T_e \sim 0.2$ eV), dense ($N_e = 10^{16}$ – 5×10^{16} cm⁻³) cesium plasmas were produced by irradiation of the vapor with a 25-ns, 10^9 -W·cm⁻² dye-laser beam operated between 6000 and 6400 Å.^{4,5} Hotter (0.3–1 eV), more-Debye plasmas were obtained by two-photon ionization of cesium atoms using a 30-ns, 10^8 – 10^{10} -W·cm⁻² frequency-doubled Nd:glass-laser beam ($\lambda = 5266$ Å). Further details of the ionization mechanisms and extensive diagnosis of N_e and T_e by emission spectroscopy can be found in Ref. 5. The frequency-doubled Nd:glass-laser wavelength was also used for scattering since cesium has a convenient minimum in its dimer absorption⁶ and emission spectrum⁷ at 5300 Å.

The light scattered at 90° was imaged onto the horizontal slits of an $f/4.2$ grating spectrometer (Bentham M300) coupled to an RCA C31034A photomultiplier and Tektronix 466 storage oscilloscope. This provided 2–3-Å, 15-ns resolution of the 0.5-cm by 100-μm plasma area viewed. Scattered spectra were recorded on a shot-to-shot basis. A series of movable mirrors allowed the cesium vapor to be pumped with either the dye laser, the Nd:glass laser, or with both by introduc-

tion of a 15-ns delay of the Nd:glass-laser beam.

The first scattering experiments were recorded with use of only one 0.1–1-MW 5266-Å beam which both ionized and scattered. The results for the “electron feature” for an initial cesium density of $(3.5 \pm 0.5) \times 10^{16}$ cm⁻³ at three progressively decreasing laser fluxes I are shown in Figs. 1(a)–1(c). The background light consisting of unrejected stray laser light and continuum radiation has been subtracted. The peak single-to-background ratios for the three cases are 10, 5, and 2, respectively. Each experimental point represents a 3 to 7 shot average. The theoretical fits shown by the dashed lines, which include the instrument function [full width at half maximum (FWHM) = 2.5 Å] and laser bandwidth (FWHM = 2.5 Å), are derived from the usual collisionless theory.⁸ The plasma parameters deduced from the scattered spectra are shown in Table I, where α , the scattering parameter, is $\lambda_{\text{laser}}/\pi\sqrt{8}\lambda_D$. Unfortunately, no comparison can be made with the results from emission spectroscopy⁵ since line-shape distortions and non-equilibrium level populations occur during strong laser irradiation. An absolute calibration of the detection system yielded $N_e = (3 \pm 1) \times 10^{16}$ cm⁻³ which agrees with the density deduced from the scattered spectral shapes.

The reduction in temperature with decreasing laser flux observed for nearly constant N_e illustrates the importance of inverse bremsstrahlung heating. The electron heating rate is given by⁹

$$\frac{dT_e}{dt} = \frac{10^{-18} I \lambda^2 N_e}{T_e^{3/2}} g, \quad (1)$$

where I , T_e , N_e , and λ are in watts per square centimeter, electronvolts, inverse cubic centimeters and micrometers, respectively, and g the free-free Gaunt factor is between 1 and 1.5 here.¹⁰ For an initial photoelectron temperature of 0.54 eV and with use of the electron density and laser flux listed in the first row of Table I, Eq. (1) predicts $T_e = 0.8$ eV within 10 ns, in reasonable agreement with the temperature measured by laser scattering. Unfortunately, the laser flux could not be further decreased in this experiment to reduce

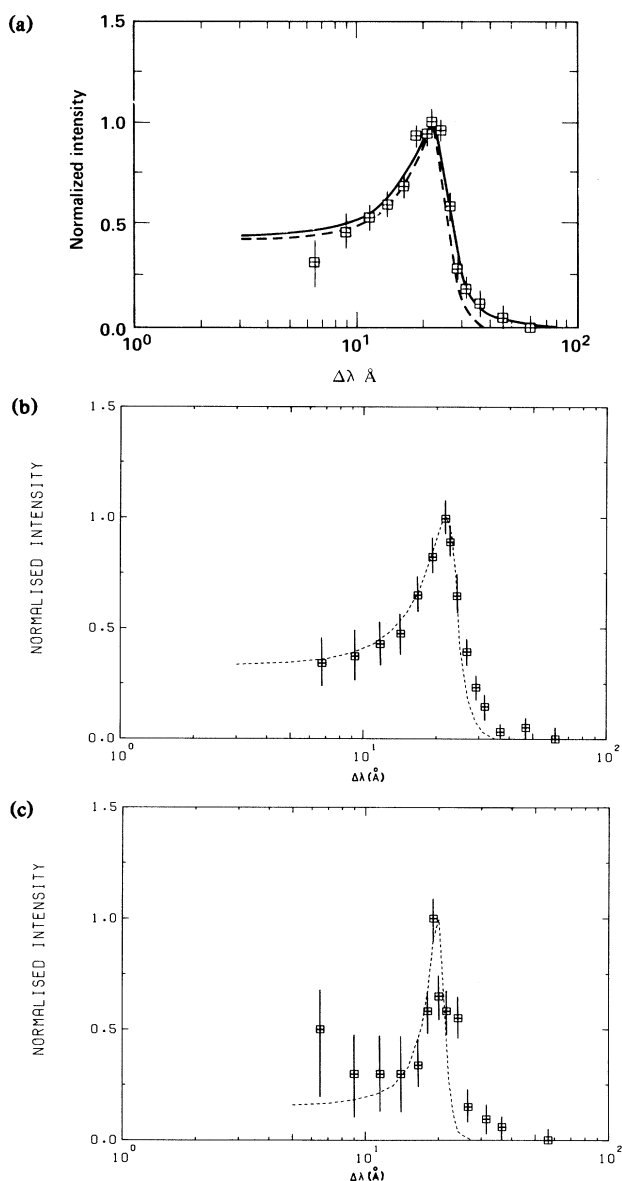


FIG. 1. (a) Electron feature of scattered spectrum fitted by $\alpha = 1.55 \pm 0.05$ of collisionless theory (Ref. 8), dashed line, and $\alpha = 1.55$, $c_e = 0.1$ of collisional theory (Ref. 14), solid line. (b) Electron feature of scattered spectrum fitted by $\alpha = 1.7 \pm 0.05$ of collisionless theory (Ref. 8). (c) Electron feature of scattered spectrum fitted by $\alpha = 2.2 \pm 0.1$ of collisionless theory (Ref. 8).

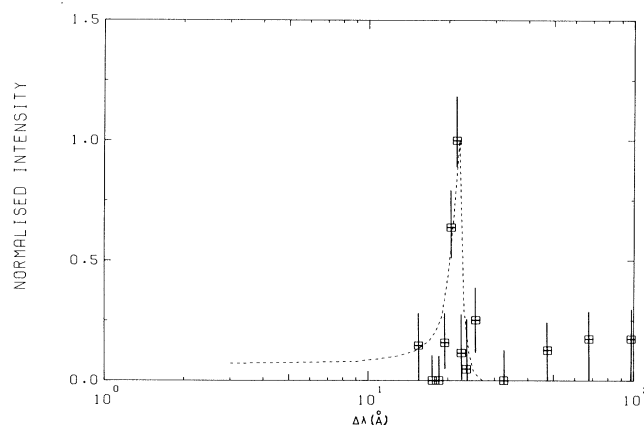


FIG. 2. Electron feature of scattered spectrum fitted by $\alpha = 3$ of collisionless theory (Ref. 8).

the heating and the number of electrons per Debye sphere because this was accompanied by a decrease in electron density and hence an even greater decrease in the number of scattered photons.

To overcome this problem, a second experiment was performed which used the dye laser beam for ionization and the 5266-Å beam for scattering with a 15-ns delay. A laser flux of 30 MW cm^{-2} was chosen for the 5266-Å beam to limit its perturbing influence on the performed plasma to an acceptable 20% increase in fluorescence. Figure 2 shows the scattered spectrum for a cesium density of $2 \times 10^{17} \text{ cm}^{-3}$, fitted by the collisionless theory. Since the width of this satellite at $\approx \omega_p$ (the plasma frequency) detuning was approximately equal to the spectral resolution, 3.5 Å, only a minimum α of 3 can be assigned, yielding $N_e = (5-6) \times 10^{16} \text{ cm}^{-3}$, a maximum $T_e = 0.36 \text{ eV}$, and hence a maximum $N_D = 1.6$, in good agreement with results from emission spectroscopy.⁵ Since the satellite spectral position is proportional to $N_e^{1/2}$, the maximum width of the satellite also sets a limit of 10% on possible large scale ($> \lambda_D$) variations in density in the plasma volume imaged. Such density inhomogeneities were thought to contribute to the anomalously large satellite widths observed in previous high- α scattering experiments.¹¹

However, for the nearly fully ionized plasmas of Table I, laser-flux inhomogeneities will create tem-

TABLE I. Results of laser scattering shown in Figs. 1(a)–1(c).

α	$I \text{ (GW cm}^{-3}\text{)}$	$N_e \text{ (cm}^{-3}\text{)}$	$T_e \text{ (eV)}$	N_D
1.55 ± 0.05	1.5	$3.5 \pm 0.2 \times 10^{16}$	0.9 ± 0.05	7.8 ± 0.09
1.70 ± 0.05	0.7	$3.5 \pm 0.2 \times 10^{16}$	0.78 ± 0.04	6.3 ± 0.06
2.2 ± 0.1	0.3	$3.15 \pm 0.3 \times 10^{16}$	0.42 ± 0.04	2.6 ± 0.05

perature rather than density variations. The wings of the satellites at large detunings ($> 20 \text{ \AA}$) shown in Figs. 1(a)–1(c) which deviate from the theoretical curves could then be explained by lower- α scattering from higher-temperature fully ionized regions, but *only* if these exceed 2 eV.

It is unlikely, however, that this explanation can account for all three wings of Figs. 1(a)–1(c) since the laser flux was decreased by a factor of 7.5 between Figs. 1(a) and 1(c).

Moreover, collisions alter the scattered spectra as either the non-Debye limit is approached¹² ($N_D < 1$) or as α becomes large.¹³ For $1 < \alpha < 3$, Lorentzian wings due to collisional damping become observable on the electron feature for

$$c_e = \nu_e \alpha / \omega_p \geq 0.05,$$

where c_e represents a ratio of collision frequency ν_e to electron plasma frequency ω_p .^{14,15} Both electron-neutral^{14,15} and electron-ion¹² collisions can contribute. However, electron-ion collisions^{16,17} will dominate in the present plasmas investigated by laser scattering, and should be observable since $c_e = 0.11, 0.17, 0.34$, and 0.69 for the cases $\alpha = 1.55, 1.70, 2.2$, and 3 , respectively. The solid curve in Fig. 1(a) represents a better theoretical fit by including such collisions¹⁴ for $\alpha = 1.55$ and $c_e = 0.1$. The range in c_e over which the theoretical curve would be within the experimental errors is 0.05 – 0.13 . However, further experiments using two different \mathbf{k} scattering vectors for the same plasma are desirable to distinguish between the effects of temperature variations and collisional damping on the scattered spectra. Nevertheless, as expected theoretically,¹² it seems clear that the classical theory⁸

$$\sigma_R = 6.6 \times 10^{-25} \sum_{j=1/2, 3/2} \left[\frac{f_{6s_{1/2}-6p_j} \lambda_{6s_{1/2}-6p_j}^2}{\lambda_{\text{laser}}^2 - \lambda_{6s_{1/2}-6p_j}^2} \right]^2 = 1 \times 10^{-24} \text{ cm}^2 \quad (2)$$

for $f_{6s_{1/2}-6p_{3/2}} = 0.814$ and $f_{6s_{1/2}-6p_{1/2}} = 0.394$. Hence, the ratio of Rayleigh component to ion feature is given by the following equation, valid for $T_e/T_{Cs+} \leq 15$ in cesium¹⁸:

$$\frac{\sigma_R}{\alpha_{Cs+}} = \frac{1.5(1 + \alpha^2)(1 + \alpha^2 + \alpha^2 T_e/T_{Cs+})}{\alpha^4}.$$

For the three cases $\alpha = 1.55, 1.7$, and 2.2 , this ratio is between 15 and 30. Thus, it is conceivable that Rayleigh scattering from the lower-fractional-ionization regions of the plasma created by the lower-intensity spatial wings of the laser beam can explain the large scattered signals observed at the laser wavelength.

This process will need to be considered when analyzing scattered spectra in the visible region from any alkali-metal and alkaline-earth vapor plasmas.

We thank Dr. J. D. Kilkenny for useful suggestions.

TABLE II. Comparison of scattered-light intensity at laser wavelength to intensity expected for the ion feature.

α	T_e/T_{Cs+}	$I_{\text{experiment}}$	I_{theory}
1.55	10–18	370 ± 50	80 ± 15
1.7	8–15	270 ± 50	60 ± 20
2.2	6–8	310 ± 50	40 ± 10

does not breakdown substantially at the electron feature for N_D as low as 1.6 and $\alpha = 1.3$.

The light scattered at the laser frequency was recorded over five to ten shots, averaged, and subtracted from the stray laser-light level. This will contain the spectrally integrated “ion feature” whose calculated half-width of 0.15 to 0.3 \AA is much smaller than the 2-\AA resolution of the detection system. The results are shown in Table II together with the theoretical predictions based on the measured intensity of the electron feature and accounting for nonequal ion (T_{Cs+}) and electron temperatures¹⁸ due to the long (200 – 400 ns) thermalization times.¹⁶ The discrepancy between theory and experiment is a factor of 10 larger than, for example, the predicted 60% increase in the intensity of the ion feature in a non-Debye plasma at $\alpha = 1$, $N_D = 0.5$.¹⁹

The more probable explanation for the enhanced scattering is Rayleigh scattering from the blue wings of the $6s$ – $6p$ resonance transition at 8943 and 8521 \AA . Ignoring collisional redistribution of radiation at more than 3000-\AA detuning from line center, the Rayleigh scattering cross section is given by²⁰

This work was supported by a Science and Engineering Research Council grant.

^(a)Present address: Lawrence Livermore National Laboratory, P. O. Box 808, Livermore, Cal. 94550.

^(b)Present address: British Aerospace, Bristol, England, P.O. Box 5, Filton, Bristol, BS12 7QW, United Kingdom.

¹D. E. Evans and J. Katzenstein, Rep. Prog. Phys. **32**, 207 (1969).

²A. Kopystynska and L. Moi, Phys. Rep. **92**, 137 (1982).

³JANAF Thermochemical Tables (National Bureau of Standards, Washington, D. C., 1971).

⁴A. C. Tam and W. Happer, Opt. Commun. **21**, 403 (1977).

⁵O. L. Landen and R. J. Winfield, to be published.

⁶M. Lapp and L. P. Harris, J. Quant. Spectrosc. Radiat.

Transfer **6**, 169 (1966).

⁷J. Huennekens, Z. Wu, and T. G. Walker, Phys. Rev. A **31**, 196 (1985).

⁸E. E. Salpeter, Phys. Rev. **120**, 1528 (1960).

⁹K. W. Billman and J. R. Stallcop, Appl. Phys. Lett. **28**, 704 (1976).

¹⁰J. R. Stallcop and K. W. Billman, Plasma Phys. **16**, 1187 (1974).

¹¹H. Rohr, Z. Phys. **209**, 295 (1968); P. W. Chan and R. A. Nodwell, Phys. Rev. Lett. **16**, 122 (1966).

¹²R. Cauble and D. B. Boercker, Phys. Rev. A **28**, 944 (1983); E. J. Linnebur and J. J. Duderstadt, Phys. Fluids **16**, 665 (1973).

¹³A. N. Mostovych and A. W. DeSilva, Phys. Rev. Lett. **53**, 1563 (1984).

¹⁴J. Kopainsky and F. Vilsmeier, Appl. Phys. **8**, 223 (1975).

¹⁵I. Gorog, Phys. Fluids **12**, 1702 (1969).

¹⁶L. Spitzer, Jr., and R. Harm, Phys. Rev. **89**, 977 (1952).

¹⁷J. P. Hansen and I. R. McDonald, Phys. Lett. **97A**, 42 (1983).

¹⁸J. Sheffeld, *Plasma Scattering of Electromagnetic Radiation* (Academic, New York, 1975).

¹⁹D. B. Boercker, R. W. Lee, and F. J. Rogers, J. Phys. B **16**, 3279 (1983).

²⁰A. Dalgarno, J. Opt. Soc. Am. **53**, 1223 (1963).